Title
Development and validation of a critical gradient energetic particle driven Alfven eigenmode transport model for DIII-D tilted neutral beam experiments

Journal
Nuclear Fusion, 55(12)

ISSN
0029-5515

Authors
Waltz, RE
Bass, EM
Heidbrink, WW
et al.

Publication Date
2015-11-01

DOI
10.1088/0029-5515/55/12/123012

IOP Publishing | International Atomic Energy Agency Nuclear Fusion

Nucl. Fusion **55** (2015) 123012 (9pp) doi:10.1088/0029-5515/55/11/123012

Development and validation of a critical gradient energetic particle driven Alfven eigenmode transport model for DIII-D tilted neutral beam experiments

R.E. Waltz[1], E.M. Bass[2], W.W. Heidbrink[3] and M.A. VanZeeland[1]

[1] General Atomics, San Diego, CA, USA
[2] University of California San Diego, San Diego, CA, 92093, USA
[3] University of California Irvine, Irvine, CA, 92697, USA

E-mail: waltz@fusion.gat.com

Received 18 June 2015, revised 6 August 2015
Accepted for publication 12 August 2015
Published 30 October 2015

Abstract

Recent experiments with the DIII-D tilted neutral beam injection (NBI) varying the beam energetic particle (EP) source profiles have provided strong evidence that unstable Alfven eigenmodes (AE) drive stiff EP transport at a critical EP density gradient [Heidbrink *et al* 2013 *Nucl. Fusion* **53** 093006]. Here the critical gradient is identified by the local AE growth rate being equal to the local ITG/TEM growth rate at the same low toroidal mode number. The growth rates are taken from the gyrokinetic code GYRO. Simulation show that the slowing down beam-like EP distribution has a slightly lower critical gradient than the Maxwellian. The ALPHA EP density transport code [Waltz and Bass 2014 *Nucl. Fusion* **54** 104006], used to validate the model, combines the low-n stiff EP critical density gradient AE mid-core transport with the Angioni *et al* (2009 *Nucl. Fusion* **49** 055013) energy independent high-n ITG/TEM density transport model controling the central core EP density profile. For the on-axis NBI heated DIII-D shot 146102, while the net loss to the edge is small, about half the birth fast ions are transported from the central core $r/a < 0.5$ and the central density is about half the slowing down density. These results are in good agreement with experimental fast ion pressure profiles inferred from MSE constrained EFIT equilibria.

Keywords: energetic particles, Alfven eigenmodes, critical gradient, transport

(Some figures may appear in colour only in the online journal)

1. Introduction

Recent experiments with the tilted DIII-D (off-axis) neutral beam injection (NBI), which significantly vary the beam energetic particle (EP) source profiles, have provided strong evidence that unstable Alfven eigenmodes (AE) drive stiff EP transport at a critical EP density gradient [1]. The experimentally inferred EP density profiles were found to be insensitive to the NBI deposition profile. We propose to identify the critical gradient with the condition that the maximum local AE growth rate exceeds the local ion temperature gradient-trapped electron mode (ITG/TEM) growth rate at the same low-n toroidal mode number. This condition, or *recipe,* was supported by early fixed-gradient nonlinear local δf gyrokinetic code GYRO [2, 3] simulations with low-n AE modes embedded in high-n ITG/TEM turbulence. The simulations showed unbounded EP transport at the critical gradient [4]. This *recipe* is somewhat more optimistic than stiff EP transport at the AE marginal stability gradient used in a recent ITER projection of AE driven alpha confinement losses [5]. The marginal stability (zero AE growth rate) gradient often proves to be difficult to identify. In any case the earlier local nonlinear simulations [4] show that the low-level EP transport from the ITG/TEM micro-turbulence was only slightly increased going well beyond the low-n AE marginal gradient when the high-n micro-turbulence is large. In essence the high level high-n ITG/TEM turbulence generates a high level of $n = 0$ zonal flows which appear to nonlinearly saturate the low-n AE modes [4]. The low-n ITG/TEM growth rate is assumed to be a good representative of the zonal flow ExB shearing rate. [6] should be consulted for a general review of energetic particle physics in fusion research preparing

for burning plasma experiments. Nearly all previous gyrokinetic studies of EP driven unstable AE modes have assumed a Maxwellian velocity distribution for the EP's. The linear GYRO simulations presented here found that the slowing-down beam-like EP distribution had a slightly lower critical gradient than that from an isotropic Maxwellian.

This paper attempts to quantitatively validate the proposed AE critical gradient stiff transport model against data from the on-axis NBI DIII-D shot 146102 using the ALPHA EP density transport code [5]. This discharge was part of the on-axis to off-axis beam deposition scan carried out in [1] in which the resulting fast ion profiles were found to be relatively insensitive to the beam deposition profile. The ALPHA code combines the low-n stiff EP critical density gradient AE transport (normally most unstable at the mid-core radii) with the Angioni *et al* [7, 8] energy independent high-n ITG/TEM density transport model which controls the central core EP density profile. While the net EP confinement loss to the edge is small, for the on-axis case known to have the strongest AE amplitudes, *about half* the birth fast ions are transported from the central core $r/a < 0.5$ and redistributed to the outer radii. The central density is *about half* the classical slowing down density. This predicted central core particle loss fraction is found to be in good agreement with experimental fast ion pressure profiles inferred from MSE constrained EFIT equilibria and fast ion D-alpha measurements. Data from fast ion D-alpha (FIDA) diagnostic sensitive to the highest energy fast ions suggest a somewhat higher diffusion rate than for the bulk fast ions.

We caution that this is a first step validation of an EP critical gradient AE transport model and there are many caveats. There is the implicit assumption that the 'input' velocity space distribution (be it Maxwellian, isotropic or beam-like slowing down) is fixed and not significantly distorted by any transport process, hence the Maxwellian effective EP temperature is unchanged. The logarithmic gradient of the effective EP temperature is small compared to the logarithmic gradient of the of the EP density. With this, the critical EP density gradient is easily converted to the more physically relevant critical EP pressure gradient. The ALPHA code is only a density moment radial transport code. Given the EP slowing-down density (or EP birth rate source) profile, ALPHA computes the transported EP density, which is difficult to measure experimentally. However, the corresponding EP pressure moment profiles computed from the EP density and fixed EP effective temperature profiles can be compared directly with experimental EP pressure profiles. When the EP beta fraction is high (>50% as in the case here), NBI fast ion pressure profile from MHD equilibrium EFIT [9, 10] reconstruction (using magnetics, motional Stark effect, thermal pressure data, etc.) is the most robust experimental EP profile data. In contrast, the fast-ion D-alpha (FIDA) diagnostic [11–13] samples a smaller portion of energy and pitch angle space. Comparative analysis of FIDA data actually requires a kinetic transport code (like TRANSP-NUBEAM [14]) with a velocity space dependent *effective diffusivity*.

However, as an EP density transport code, ALPHA assumes a velocity space (energy and pitch angle) independent *effective diffusivity*. The EP *effective diffusivity* is a function of the radius only independent of energy (and pitch angle). In essence the EP energy transport flux is assumed to be purely convective with $Q_{EP} = (3/2)T_{EP}\Gamma_{EP}$. While the low-n AE stiff critical gradient energy transport is likely somewhat stronger than purely convective [5], EP transport from the high-n ITG/TEM can be considerably less when the EP temperature T_{EP} is much larger than the electron temperature T_e [7, 8]. For the case of fusion alphas in a burning plasma where $T_{EP}/T_e \sim O(100)$, the ITG/TEM energy transport flux can be 1/30 the purely convective flux [5]. For the central core where ITG/TEM transport is most important in the DIII-D NBI case at hand $T_{EP}/T_e \sim O(10)$, the energy flux for the Angioni model [7] is about 1/3 the purely convective flux. By treating only the EP particle density transport, the ALPHA code correspondingly overestimates the measurable EP pressure transport in the central core, where high-n ITG/TEM transport is dominant, while perhaps underestimating the mid-core low-n AE transport. It is important to note that any critical gradient model of low-n AE EP transport cannot be validated independent of a model for the ITG/TEM EP transport.

Section 2 of the paper provides some details of the experimental and simulation profile parameters for the DIII-D shot 146102 tilted NBI series. Section 3 illustrates the construction of our *recipe* for the local critical EP density gradient profile from local linear GYRO simulations. Predictions from Maxwellian, isotropic and beamlike slowing down distributions are compared. Section 4 illustrates the application of the *recipe* in the ALPHA EP density transport code and our best attempts to validate the *recipe*. For convenience of the reader, the appendix summarizes (and corrects) the formulation of the ALPHA code first given in [5] and the Angioni model [7].

2. Experimental and simulation profile parameters

This paper focuses on the 1 MA current 2 T toroidal field L-mode DIII-D on-axis NBI discharge 146102 of [1]. The safety factor at $r/a = 0.0,\ 0.5,$ and 1.0 is $q(0.0,\ 0.5,\ 1.0) = (5.2, 4.5, 8.7)$ respectively. The major radius is $R(0.0,\ 1.0) = (1.7, 1.6)$m with a flat elongation $\kappa(0.0, 1.0) = (1.72, 1.66)$. The mid-plane minor radius is $a = 0.61m$. This discharge is in a series with increasing off-axis beam-mix fractions [0.0, 0.22, 0.45, 0.75, 1.0] at a fixed 4MW power (with the latter far off-axis discharge 146101). It is assumed that the discharge parameters and thermal plasma profiles (figure 2 of [1]) do not significantly vary in the series. Rather, there is an extreme variation in the NBI deposition with the classical (no transport) slowing-down beam density computed from TRANSP NUBEAM [14] peaking to $n_{EP}(0) = 0.42 \times 10^{19}\mathrm{m}^{-3}$ at the center in the on-axis case and peaking at mid-core $n_{EP}(0.4) = 0.12 \times 10^{19}\mathrm{m}^{-3}$ in the extreme off-axis case (see figure 4 [1]). In the on axis case, the electron density is $n_e(0.0, 0.5, 1.0) = (3.8, 2.1, 1.5) \times 10^{19}\mathrm{m}^{-3}$, the electron temperature is $T_e(0.0, 0.5, 1.0) = (1.8, 0.55.\ 0.05)$keV the ion temperature is $T_i(0.0, 0.5, 1.0) = (1.5, 0.55.\ 0.15)$keV and the ion toroidal rotation is $\Omega(0.0, 0.5, 1.0) = (55, 20, 5) \times 10^3\,\mathrm{rad\,s}^{-1}$. It should be noted that the linear GYRO

simulations, in section 3 to follow, did not include any effects of rotational or ExB shear. The $Z_{\rm eff}$ ~1.5 profile is rather flat. The key result from [1] for our interest here is that the 'FIDA density' profile was invariant to the NBI deposition profile for the beam-mix less than 0.75, where the AE modes were unstable (see figure (10) of [1]). This invariance is a signature of a critical gradient in the EP density, which we hope to quantify.

The TRANSP NUBEAM code [14] used to obtain the classical (no transport) slowing down EP density used the full, half, and third components of the nominal 80 keV beams. The NUBEAM-generated equivalent EP temperature is $T_{\rm EP}(0.0, 0.5, 1.0) = (22, 18, 9.1)$keV. The effective temperature profile is well matched by a single component injection energy $E_{\rm EP} = 64$keV for the isotropic slowing down distribution used in the GYRO (and ALPHA) codes: $\widehat{F}_s(\widehat{E}) = \{1/[\widehat{E}_c^{3/2} + \widehat{E}^{3/2}]\}/I_2(\widehat{E}_c^{1/2})$ where $\int_0^1 \widehat{E}^{1/2} d\widehat{E}\, 2\widehat{F}(\widehat{E}) = 1$ and $I_2(\widehat{E}_C^{1/2}) = \int_0^1 \widehat{E}^{1/2} {\rm d}\widehat{E}/2\{1/[\widehat{E}_c^{3/2} + \widehat{E}^{3/2}]\} = (1/3)1n[(1 + \widehat{E}_C^{3/2})/\widehat{E}_C^{3/2}]$ with $\widehat{E} = E/E_{\rm EP}$ and $\widehat{E}_c$ the similarly normalized cross-over energy. For the beam-like slowing down distribution, an all co-current single pitch angle $\xi = v_{||}/v = \sqrt{1 - \lambda\widehat{B}}$ distribution was used: $F_{\rm bpa}({\rm co}, \lambda\widehat{B}) = \exp[-(\Lambda - \Lambda_0)^2/\Lambda\Delta^2]/\{1/2\int_0^1 {\rm d}\bar{\xi}/\bar{\xi}^{1/2} \exp[-(\bar{\xi} - \xi_0)^2/\Delta\xi^2]\}$ and $F_{\rm bpa}({\rm ctr}, \lambda\widehat{B}) = 0$ where $\Lambda = 1 - \xi^2$, $\lambda\widehat{B} = \Lambda_0 = 0.5$, $\Delta\lambda\widehat{B} = \Delta\Lambda = 0.2$ and hence $\xi_0 = 0.707$, $\Delta\xi = \Delta\Lambda/(2\xi_0) = (0.2/1.41) = 0.1414$. At $r/a = 0.5$ the trapped-passing boundary is at $\lambda\widehat{B} = 0.69$ at which point the EPs are mostly passing. The reformulation of GYRO to handle beam-like slowing down distributions followed the Antonsen and Lane [15] formulation of gyrokinetics for a general distribution to write $-\partial 1nF/\partial E|_\mu$ and $-\partial 1nF/\partial\mu B|_E$ with $\mu = \lambda/E$. The rather complicated modifications to the GYRO field solve equations had little effect on stability since the EP density relative to the thermal plasma density is small, hence the change in net polarization density is small.

3. Construction of the critical gradient model from local mode linear stability

To construct our *recipe* for the critical EP density gradient, we first look at the global mode growth rates from GYRO linear initial value simulations with a Maxwellian EP distribution using the experimental slowing down EP density profile for DIII-D discharge 146102 described in section 2. The discharge with a high minimum-q can drive reverse shear Alfven eigenmodes (RSAEs). However the most unstable global mode spanning mid-core to the outer radii and surviving to the weakest off -axis heating driving gradient is a toroidal Alfven eigenmode (TAE). The relative amplitudes and radial location of the four leading global eigenmodes are shown in figure 11 of [1]. The sub-dominant global eigenmodes localized to the inner core radii are unstable only for the strongest

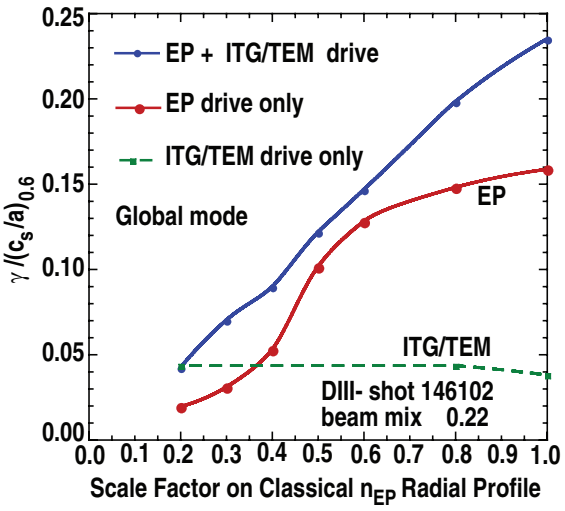

Figure 1. Global mode growth rates normed at $r/a = 0.6$versus the scale factor S_F on the experimental slowing down EP density profile for DIII-D shot 146102 beam mix 0.22. Maximum amplitude at $r/a = 0.54$. Isotropic Maxwellian NBI energetic particle distribution.

driving gradients with on-axis heating. Initial value simulations pick-up only the mode unstable mode. Figure 1 shows the most unstable $n = 3$ *global* mode rates (normed to $[c_s/a]$ at $r/a = 0.6$) as the experimental EP slowing down density profile is scaled downward by a scale factor $S_F = n_{\rm EP}(r)/n_{\rm EP}^{\rm exp}(r)$. $c_s = \sqrt{T_c/m_i}$ is the local sound speed. The global growth rates have a broad maximum over n = 3, 4, and 5. Assuming lower wave numbers have longer mixing lengths, we take $n = 3$ to be the most important in determining the critical gradient. The key question is whether to identify the critical gradient with the $\gamma_{\rm AE} > 0, \gamma_{\rm AE+ITG/TEM} > \gamma_{\rm ITG/TEM}$, or $\gamma_{\rm AE} > \gamma_{\rm ITG/TEM}$. Figure 1 shows that the corresponding threshold scale factors S_F are roughly (extrapolated to) 0.0, 0.2, 0.35 respectively. The subscript AE (ITG/TEM) refers to the EP driving gradients on (off) and the thermal plasma driving gradients off (on). AE+ITG/TEM refers to both EP and thermal plasma gradients turned on. The most unstable global AE mode amplitudes maximize at about $r/a = 0.54$ which is close to the minimum-q.

A *local* critical gradient model is most conveniently determined from the most unstable *local* eigenmode growth rates. That is fortunate since we argue that local modes are more relevant to profile gradient relaxation to a critical gradient than global modes. Local modes need only phase correlate a few near-by singular surface. They are quicker to form. The phase correlation over many singular surfaces required of global modes means they are slower to form and easily broken up in a background of high-n turbulence. In fact at the radial location of maximum amplitude for any global mode (even a sub-dominant global mode), the local mode will have the higher growth rate since they suffer less from plasma profile shear stabilization. Referring again to figure 11 of [1], local modes can also 'feed' the central core sub-dominant global modes as well as the most unstable mid to outer core global mode treated in figure 1.

Local growth rates are shown in figure 2 for $r/a = 0.3$, 0.4, 0.5, and 0.6. At full driving $S_F = 1$, the strongest local

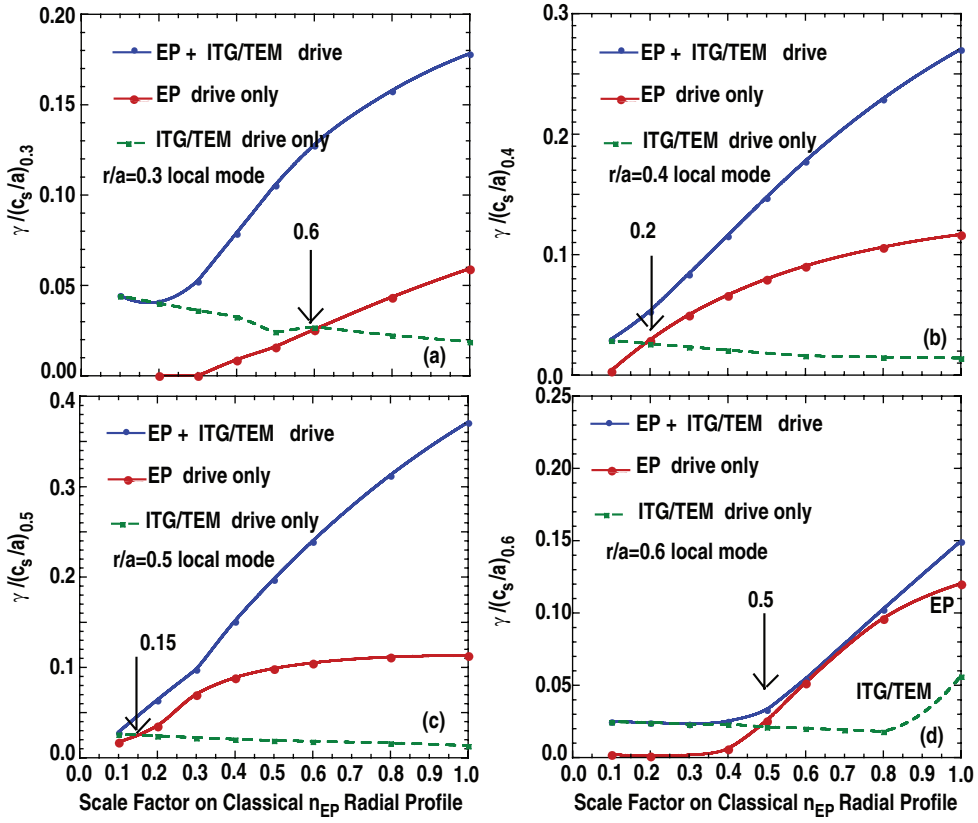

Figure 2. Local mode growth rates versus the scale factor S_F on the experimental the slowing down EP density profile at $r/a = 0.3$ in (a), 0.4 in (b), 0.5 in (c), and 0.6 in (d) for DIII-D shot 146102 beam mix 0.22. Isotropic Maxwellian NBI energetic particle distribution.

mode growth rate $\gamma_{AE+ITG/TEM} = 0.41[c_s/a]_{0.6}$ is at $r/a = 0.5$ shown in figure 2(c). As expected the maximum local growth rate it is considerably larger than the corresponding global rate $\gamma_{AE+ITG/TEM} = 0.23[c_s/a]_{0.6}$ shown in figure 1. Away from the maximum [e.g. $r/a = 0.6$ figure 2(d)], the local growth rate $\gamma_{AE+TEM} = 0.12[c_s/a]_{0.6}$ can be lower than the global growth rate. More importantly, the scale factor for $\gamma_{AE} > \gamma_{ITG/TEM}$ at the maximum local rate near $r/a = 0.5$ is $S_F = 0.15$ [figure 2(d)] compared to $S_F = 0.35$ in the global mode case [figure 1]. The critical EP density (pressure) gradient is given by the scale factor times the slowing down density (pressure). As can be seen from figure 2, the scale factors for $\gamma_{AE+ITG/TEM} > \gamma_{ITG/TEM}$ are about 20%, 30%, 50%, and 60% lower than for our chosen *recipe* $\gamma_{AE} > \gamma_{ITG/TEM}$ at $r/a = 0.6$, 0.5, 0.4 and 0.3 respectively. The corresponding critical gradients will be somewhat lower and in the central core $r/a < 0.3$ perhaps considerably lower. Computationally intensive nonlinear GYRO simulations of the DIII-D analogous to [4] with low-n AE modes embedded in high-n ITG/TEM turbulence are in progress to determine which condition $[\gamma_{AE+ITG/TEM} > \gamma_{ITG/TEM}$ or $\gamma_{AE} > \gamma_{ITG/TEM}]$ more accurately represents the critical gradient defined by unbounded EP transport at fixed gradients. At $r/a = 0.6$, 0.4, and 0.3 the marginal stability point $\gamma_{AE} > 0$ appears to coincide with the $\gamma_{AE+ITG/TEM} > \gamma_{ITG/TEM}$. However, as discussed in [5], determination of any the marginal point ($\gamma_{AE} > 0$ γ_{AE} or $\gamma_{AE+ITG/TEM} > 0$) required higher GYRO grid resolution and in general is not always clear.

Figure 3 contrasts the γ_{AE} and $\gamma_{ITF/TEM}$ growth rates versus the scale factor S_F on the experimental slowing down EP density from Maxwellian, isotropic slowing down, and beam-like slowing down EP velocity distributions. Global mode growth rates are shown in figure 3(a) and the most unstable $r/a = 0.5$ local mode growth rates in figure 3(b). Figure 3(c) shows the corresponding critical EP density gradients in comparison to the classical slowing down EP gradient (labeled experiment.) The critical gradients are lower with increasing free energy in the EP velocity space distribution function. Note that figure 3 (and the earlier figures) refer to beam-mix fraction 0.22, but the critical gradients are insensitive to beam-mix in the DIII-D 146102 series since the thermal plasma and equilibrium are not significantly different.

4. Validation of the critical gradient model

To validate the AE critical EP density gradient profiles determined from the GYRO linear growth rates, the critical profiles are inserted in the ALPHA EP density transport code reviewed in the appendix. Figure 4 illustrates the beam-mix 0.0 on-axis deposition case. Figure 4(a) shows that with the Angioni energy independent EP transport model [7, 8] for the high-n ITG/TEM micro-turbulence acting alone (labeled AE off) there is only a small reduction of the central density from the slowing down. Figure 4(d) indicates that only about 10% of the particle birth flow is lost from the mid-core at $r/a = 0.5$. This is in contrast to the effect

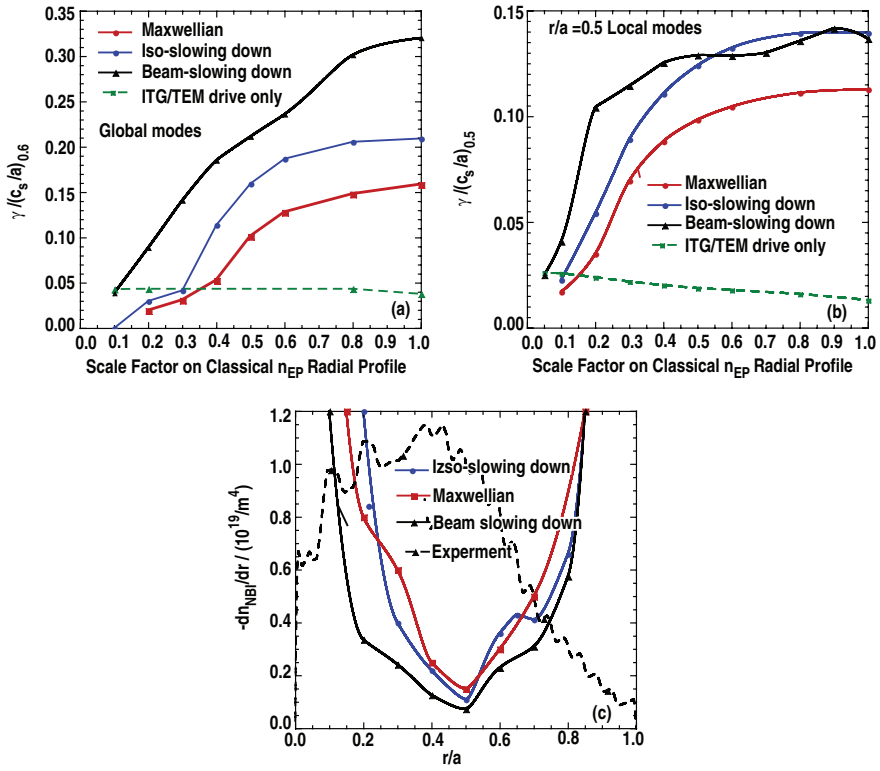

Figure 3. Global mode growth rates (*a*) and local mode growth rates (*b*) versus the scale factor S_F on the slowing down EP density profile. Experimental slowing down EP density gradient (black dashed) and critical density gradients in (*c*) comparing Maxwellian (red circle), isotropic slowing down (blue square), and beam-like slowing down (black triangle) NBI energetic particle velocity distributions for DIII-D shot 146102 beam-mix 0.22. 'Experimental' EP density from TRANSP.

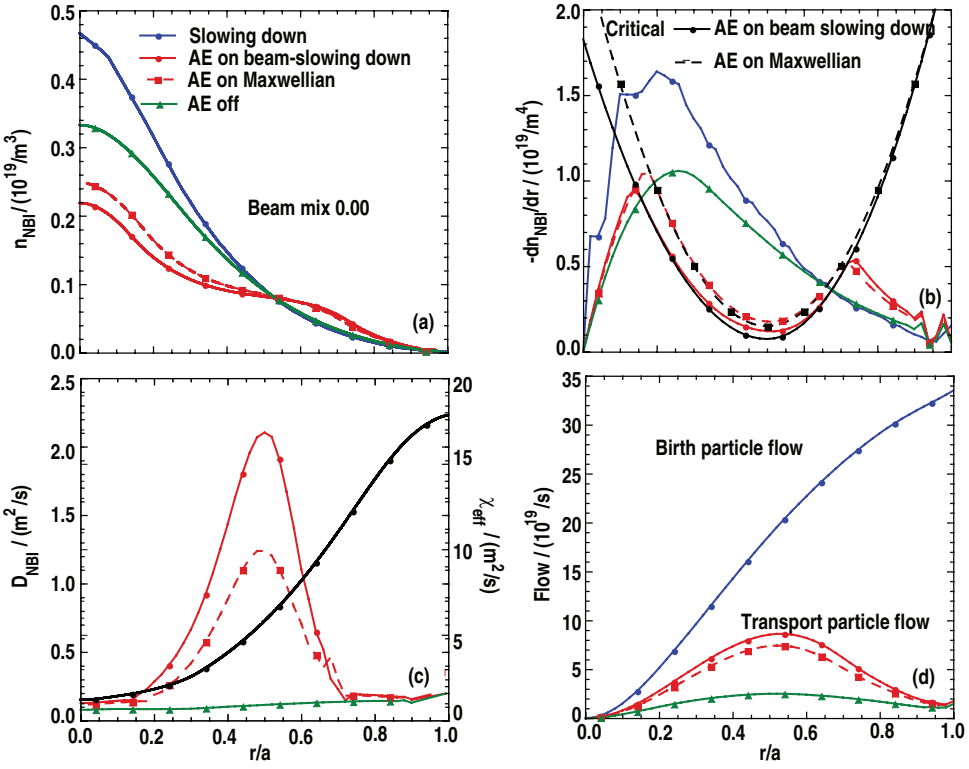

Figure 4. EP density profiles in (*a*), EP density gradient profiles in (*b*), EP effective diffusivity and plasma effective diffusivity profiles in (*c*), with birth and transport particle flows profiles in (*d*) versus normalized radius for DIII-D shot 146102 (on-axis) beam mix 0.0. Examples with AE transport 'off' and 'on' comparing Maxwellian and beam-like slowing down NBI velocity distributions are shown.

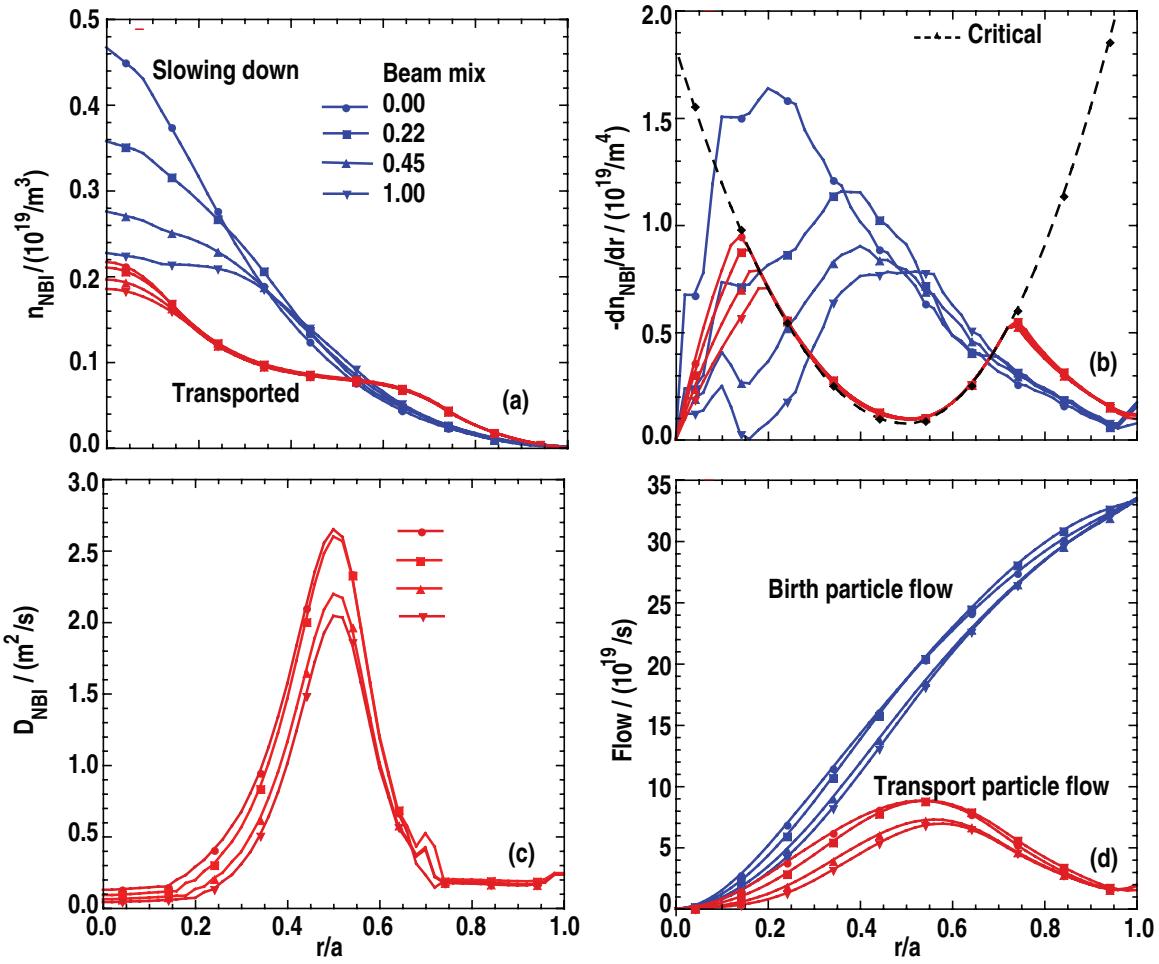

Figure 5. EP density profiles in (*a*), EP density gradient profiles in (*b*), EP effective diffusivity and plasma effective diffusivity profiles in (*c*), with birth and transport particle flows profiles in (*d*) versus normalized radius for DIII-D shot 146102 increasingly off-axis beam mix 0.0–1.0 using the beam-like slowing down NBI velocity distribution critical gradient.

of adding the AE stiff transport (AE on) at mid-core: the fully transported peak EP density is *about half* the slowing down peak [figure 4(*a*)] and *about half* the birth particle flow is lost from the mid-core $a/r = 0.5$ [figure 4(*d*)]. Note the 'redeposition effect' in figure 4(*d*) where the transported particle flow decreases to a small level beyond the mid-core. We stress again that any low-n AE critical gradient model cannot really be validated independent of a model for the high-n ITG/TEM transport of EPs. Since the AE stiff transport does not (in this case) penetrate to the central core, the central peak EP density would be much high without the ITG/TEM transport [see figure 4(*a*)]. Figure 4(*b*) illustrates the AE transported EP density gradient is driven close to the critical gradient where the slowing down EP gradient exceeds the critical. The 'over shoot' at $0.65 < r/a < 0.75$ beyond where the slowing down gradient exceeds the critical could be termed an AE 'avalanching' effect. This 'over shoot' is characteristic of other critical EP gradient models [16]. In very strongly driven cases, it is possible that the 'over shoot' can reach into the center and to the edge. The corresponding effective particle density (or velocity space independent) diffusivity profiles are shown in figure 4(*c*) in comparison with the thermal plasma effective energy diffusivity. Note that AE transported EP density profiles for the beam-like slowing down distribution is only slightly lower than the Maxwellian. The distinction is not likely within the resolution of the experimental uncertainty. These simulations are not inconsistent with previous DIII-D experimental results which found that EP transport enhancement due to microturbulence to be below detectable levels and EP transport from coherent AE's considerably larger [17] and in the range of 1 $m^2\ s^{-1}$.

Figure 5 repeats the figure 4 panels using the beam-like slowing down NBI velocity distribution only and varying the beam-mix from on-axis to off-axis: 0.0, 0.22, 0.45, 1.00. The central peak slowing down density drops by 50% [figure 5(*a*)] and the peak in the slowing down density gradient shifts outward from $r/a = 0.2$ to 0.5 [figure 5(*b*)]. [The slowing down density profiles by TRANSP NUBEAM (from which the source profiles are derived as in appendix A) were uniformly shifted up or down by as much as 8% to make sure the net birth flow to the edge is exactly the same as shown in figure 5(*d*). In any case, it is difficult for the experiment to keep total NBI power exactly constant and figure 5 is intended as illustration.] The main point is that the transported EP density profiles in figure 5(*a*) are almost perfectly invariant: a key *qualitative* signature of a critical gradient. The predicted

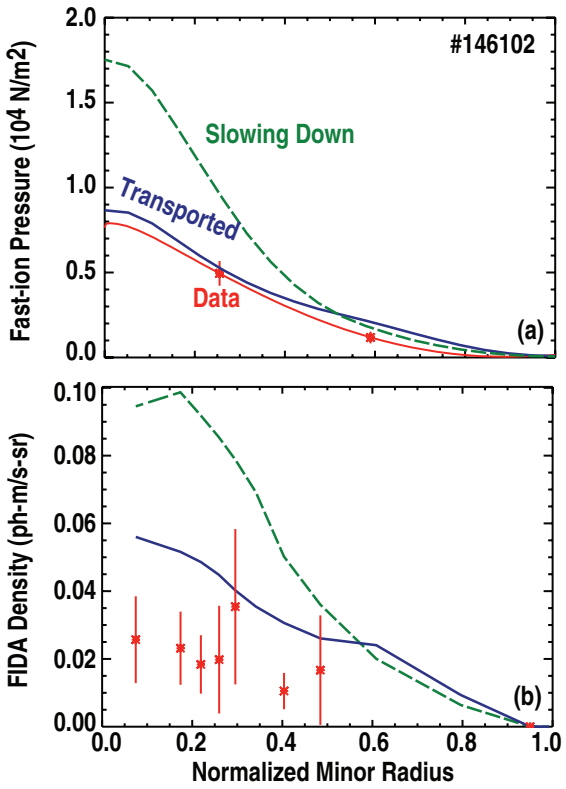

Figure 6. DIII-D shot 146102 at 545 ms on-axis NBI. (*a*) Total fast-ion pressure from MHD equilibrum EFIT [9, 10] reconstruction (from magnetics, motional Stark effect, thermal pressure data) versus normalized radius. (Representative random errors associated with uncertainties in the thermal pressure are shown for two positions; systematic errors in the equilibrium reconstruction are of comparable magnitude). (*b*) The 'FIDA density' is the FIDA brightness divided by injected neutral density versus normalized radius. FIDASIM code slowing down (dashed green), and FIDASIM code transported (solid blue) 'FIDA density' is obtained with a TRANSP code prediction from model velocity space independent effective diffusivity [figure 4(*c*)]. Experimental 'FIDA density' data (red star points) with one-sigma random error bars.

invariance is consistent with the invariance of the 'FIDA density' (see figure 10(*a*) of [1]) for beam-mix fraction <0.72 but not for extreme off-axis beam-mix of 1.0 which had substantially *lower* 'FIDA density' and also substantially *lower* AE amplitude signals (see figure 8 of [1]). The *lower* 'FIDA density' can only be explained by an under rated off-axis (tilted) beam line power which produced all the NBI power in the beam-mix 1.0 case.

Returning to the better documented on-axis beam-mix 0.0 case, a more *quantitative* measure of the critical gradient is to compare the predicted and experimental EP pressure profile as in figure 6(*a*). The slowing-down and transport EP pressure was taken directly from TRANSP NUBEAM using the velocity space independent effective diffusivity from the ALPHA code [e.g. figure 4(*c*)] in the case of the transported profile. [The 'ALPHA diffusivity' (defined the appendix) was multiplied by the appropriate geometric factor $1/\langle|\nabla r|^2\rangle \sim 1.49$ converting to 'TRANSP diffusivity'. As a code verification, TRANSP NUBEAM pressure (and density) profiles were found to be in excellent agreement with the direct predictions from ALPHA.] The MHD equilibrium EFIT [9, 10] reconstructed EP pressure profile (from external magnetics, motional Stark effect, and thermal pressure data) is considered highly reliable because the beam beta fraction is very high ($>50\%$). Very small sample error bars are indicated in figure 6(*a*). The experimentally reconstructed EP pressure is slightly lower than the reconstructed EP pressure profile 'data' and shows no evidence of the 'redeposition effect' where the transported pressure [density] in figure 6(*a*) [in figure 5(*a*)] exceeds the slowing down outside the mid-core. Otherwise it seems reasonable to conclude that the pressure profile data is consistent with the AE critical gradient prediction that transported peak EP density is *about half* the slowing down peak and *about half* the birth particle flow is lost from the mid-core.

On the other hand, the more difficult to interpret 'FIDA density' diagnostic [11–13] data in figure 6(*b*) *appears* to be more consistent with peak and mid-core losses of *about three-fourths* the slowing down density and birth. The vertical FIDA data is integrated over wavelengths from 650.5–652.7 nm, which correspond to energies along the line-of-sight of 25–68 keV. The much larger error bars [compared to the EFIT data in figure 6(*a*)] results mainly from the FIDA brightness calibration based on a comparison to an AE-quiescent discharge acquired on the same day. Recalling that the effective NBI injection energy is 64 keV and the mid-core effective EP temperature is only 9 keV (corresponding to about 15 keV energy), the FIDA diagnostic is most sensitive to transport of the high energy 'tail' EPs rather than the bulk as in the case of the pressure data. In effect the FIDA data appears to be consistent with the high energy tail having *about twice* the diffusivity of the bulk. This may be consistent with the mid-core ($r/a = 0.5$) AE transport having a 'coefficient of convection' [5] ratio $C = Q_{EP}/(3/2)T_{EP}\Gamma_{EP}$ *as large as two*. [For example in Maxwellian distribution case of figure 2(*c*), the quasilinear value of C is about 1.5 well above threshold but appear to get as large as 2.0 near threshold at $S_F = 0.2$].

5. Conclusions

Our overall conclusion is that the AE critical EP density gradient stiff EP transport model determined by the *recipe* $\gamma_{AE} > \gamma_{ITG/TEM}$ presented in section 3, is in good agreement with the NBI fast ion pressure profile inferred from MSE constrained equilibrium EFIT reconstructions for the on-axis NBI deposition DIII-D discharge 146102 [figure 6(*a*)]. The agreement is consistent with *about half* the birth fast ions lost from the central core ($r/a > 0.5$) as predicted by the ALPHA EP density transport code (reviewed in the appendix). The ALPHA code and the current critical EP density gradient model provides only a velocity space independent effective diffusivity for purely convective transport. Thus ALPHA cannot *directly* account for the FIDA diagnostic data [figure 6(*b*)] which indicates that the high energy EP 'tail' transports at *about twice* the bulk (purely convective) rate. It was found that AE quasilinear EP energy transport can be as much as *two times* larger than purely convective. Going forward, the treatment of EP transport can be improved with the use of

kinetic transport codes and the use of velocity space dependent effective diffusivity models for ITG/TEM induced EP transport; e.g. the energy dependent version of the Angioni model [7, 8], the DEP model [18], or the Pueschel model [19]. Computationally intensive nonlinear GYRO simulations of this DIII-D discharge with low-n AE modes embedded in high-n ITG/TEM turbulence in the presence of equilibrium ExB shear should provide a more accurate *recipe* for the critical gradient as well as some insight into the development of a velocity space dependent effective diffusivity for stiff critical gradient transport of EPs induced by AEs.

Acknowledgments

This material is based upon work supported by the U.S. Department of Energy, Office of Science, Office of Fusion Energy Sciences, Theory Program, using the DIII-D National Fusion Facility, a DOE Office of Science user facility, under Awards DE-FG02-95ER54309 (for theory); DE-FC02-08ER54977 SciDAC-GSEP Grant (for energetic particle simulations); and DE-FC02-04ER54698 (for DIII-D analysis). DIII-D data shown in this paper can be obtained in digital format by following the links at https://fusion.gat.com/global/D3D_DMP.

Appendix A. Formulation of the ALPHA Code

The EP density $n_{EP}(r)$ continuity equation is

$$\partial n_{EP}(r)/\partial t - 1/V'\partial[V'\, D_{EP}\partial n_{EP}(r)/\partial r]/\partial r = S_0(r)[1 - n_{EP}(r)/n_s(r)] \quad (A.1)$$

where $S_0(r) = n_S(r)/\{\tau_S(r)I_2[a(r)]\}$ and $S_0(r)[n_{EP}(r)/n_S(r)]$ is the slowing down sink. The slowing down density $n_S(r)$ is taken from the TRANSP NUBEAM [14] code. To a good approximation $V' = d[2\pi^2\kappa r R_0]/dr$. τ_S is the slowing down time, $a = \sqrt{E_c/E_{EP}} = \sqrt{\widehat{E}_c}$ is the square root ratio of the EP birth or injection energy, and $I_n(a) = \int_0^1 dx\, x^n/(a^3 + x^3)$. The Maxwellian equivalent temperature of the EP is given by $T_{EP} = (2I_4/3I_2)E_{EP}$. The standard Gaffey formulas [20] are used for the isotropic slowing down distribution. (See also equations (1)–(11) of [21].) At the edge $\hat{r} = r/a$ (actually the pedestal top) we take the boundary density condition $n_{EP}(a)/n_S(a) = d_1$ with d_1 between 0 and 1. The more pessimistic value $d_1 = 0$ corresponds to an orbit loss time much less than the slowing down and transport time at the edge. It seems unlikely that $d_1 = 1$. Without transport $D_{EP} = 0 \Rightarrow n_{EP}(r) = n_S(r)$. We are concerned here with the stationary state solutions: $\partial n_{EP}(r)/\partial t = 0$. The inner core transport has $n_{EP}(r) < n_S(r)$ and outer core redeposition has $n_{EP}(r) > n_S(r)$. A marginally stable AE alpha transport 'diffusivity' is added to the high-n micro-turbulent effective diffusivity D_{EP}:

$$D_{EP} = D_{AE}(a/n_{EP})[(-\partial n_{EP}/\partial r) - (\partial n_{EP}^{th}/\partial r)]_{>0} + D_{ITG/TEM}^{EP} \quad (A.2)$$

where $(-\partial n_{EP}^{th}/\partial r)$ is the local linear AE density critical gradient, and $[x]_{>0} = 0$ if $x < 0$. When $(-\partial n_{EP}/\partial r) > (-\partial n_{EP}^{th}/\partial r)$, $D_{AE} = 10.0 m^2\, s^{-1}$ is sufficient to drive the EP density gradient close to the critical for the DIII-D case here. As characteristic of 'stiff' critical gradient models, the resultant transport flows are insensitive to larger values.

The micro-turbulent transport of EPs is provided by the Angioni *et al* quasilinear models [7, 8] fitted to several cross verified gyrokinetic codes. The key formulas are repeated here for the convenience of the reader:

$$\Gamma_{ITG/TEM}^{EP} = -D_{ITG/TEM}^{EP} dn_{EP}/dr = n_{EP} D_{EP}^{A}[1/L_n^{EP} + C_p^{EP}/R] \quad (A.3a)$$

$$D_{EP}^{A} = \chi_{eff}[0.02 + 4.5(T_e/E_{EP}) + 8(T_e/E_{EP})^2 + 350(T_e/E_{EP})^3] \quad (A.3b)$$

$$C_p^{EP} = 3/2(R/L_{Te})\left\{1/[1 + \widehat{E}_c^{1.5}])\log(1+1/\widehat{E}_c^{1.5})\right] - 1\right\} \quad (A.3c)$$

where typically $C_p^{EP} < 0$ indicates 'thermal pinching'. The so called 'energy pinch' is dropped in the Angioni model. The base normalization has $\chi_{eff} = \chi_i + \chi_e$ corresponding the combined effective energy diffusivity of the thermal plasma when the ion and electron densities and temperatures are the same. x_{eff} it computed assuming the EP (NBI) heating is the only source:

$$\chi_{eff} = E_{EP}\Gamma_{EP}^{birth}/[(-n_i dT_i/dr - n_e dT_e/dr)/2] \quad (A.4)$$

where $\Gamma_{EP}^{birth}(r) = \int_0^r V'(\bar{r})S_0(\bar{r})d\bar{r}/V'(r)$ is the alpha birth source flux. Note that the Angioni model fitting was actually for fusion alpha particles in an effective DT plasma, but applied here to a D- NBI and thermal plasma.

References

[1] Heidbrink W.W., Van Zeeland M.A., Austin M.E., Bass E.M., Ghantous K., Gorelenkov N.N., Grierson B.A., Spong D.A. and Tobias B.J. 2013 *Nucl. Fusion* **53** 093006
[2] Candy J. and Waltz R.E. 2003 *Phys. Rev. Lett.* **91** 045001
[3] Candy J. and Waltz R.E. 2003 *J. Comp. Phys.* **186** 545
[4] Bass E.M. and Waltz R.E. 2010 *Phys. Plasmas* **17** 112319
[5] Waltz R.E. and Bass E.M. 2014 *Nucl. Fusion* **54** 104006
[6] Gorelenkov N.N., Pinches S.D. and Toi K. 2014 *Nucl. Fusion* **54** 104006
[7] Angioni C. and Peters A.G. 2008 *Plasma Phys.* **15** 052307
[8] Angioni C., Peters A.G., Pereverzev G.V., Botino A., Candy J., Dux R., Fable E., Hein T. and Waltz R.E. 2009 *Nucl. Fusion* **49** 055013
[9] Lao L.L., St John H., Stambaugh R.D., Kellman A.G. and Pfeiffer W. 1985 *Nucl. Fusion* **25** 1611
[10] Lao L.L., St John H.E., Peng Q., Ferron J.R., Strait E.J., Taylor T.S., Meyer W. H., Zhang C. and You K.I. 2005 *Fusion Sci. Technol.* **48** 763
[11] Luo Y., Heidbrink W.W., Burrell K.H., Gohil P. and Kaplin D. 2007 *Rev. Sci. Instrum.* **78** 033505
[12] Muscatello C.M., Heidbrink W.W., Taussig D. and Burrell K.H. 2007 *Rev. Sci. Instrum.* **81** 10D316
[13] Grierson B.A. *et al* 2010 *Rev. Sci. Instrum.* **83** 10D529
[14] Pankin A., Mccume D., Andre R., Batemann G. and Kritz A. 2004 *Comput. Phys. Commun.* **159** 157
[15] Antonsen T.M. and Lane B. 1980 *Phys. Fluids* **23** 1205

[16] Ghantous K., Gorelenkov N.N., Berk H.L., Heidbrink W.W., and Van Zeeland M.A. 2012 *Phys. Plasmas* **19** 092511
[17] Pace D.C. *et al* 2013 *Phys. Plasmas* **20** 056108
[18] Waltz R.E., Bass E.M. and Staebler G.M. 2013 *Phys. Plasma* **20** 042510
[19] Pueschel M.J., Jenko F., Schneller M., Hauf T., Gunter S. and Tardini G. 2012 *Nucl. Fusion* **52** 103018
[20] Gaffey J.D. Jr 1976 *J. Plasma Phys.* **16** 149
[21] Estrada-Mila C., Candy J. and Waltz R.E. 2006 *Phys. Plasma* **13** 112303